DEVELOPMENT OF A FINITE-ELEMENT-BASED DESIGN SENSITIVITY ANALYSIS FOR BUCKLING AND POSTBUCKLING OF COMPOSITE PLATES

RUIJIANG GUO and ADITI CHATTOPADHYAY

Department of Mechanical and Aerospace Engineering, Arizona State University, Tempe, AZ 85287-6106

A finite element based sensitivity analysis procedure is developed for buckling and postbuckling of composite plates. This procedure is based on the direct differentiation approach combined with the reference volume concept. Linear elastic material model and nonlinear geometric relations are used. The sensitivity analysis technique results in a set of linear algebraic equations which are easy to solve. The procedure developed provides the sensitivity derivatives directly from the current load and responses by solving the set of linear equations. Numerical results are presented and are compared with those obtained using finite difference technique. The results show good agreement except at points near critical buckling load where discontinuities occur. The procedure is very efficient computationally.

KEYWORDS: Composite plates; buckling and postbuckling; finite-element model; sensitivity analysis

1. INTRODUCTION

Design sensitivity analysis (DSA), in which derivatives of responses are calculated with respect to design variables, is necessary in optimal design process, reliability analysis, probabilistic analysis and in the determination of relative importance of design variables in structural performance. The simplest technique for DSA is the finite difference method which is often computationally prohibitive. Two alternate approaches are the direct differentiation approach (DDA) and the adjoint variable approach. The DSA using either of these two techniques can be performed either semi-analytically or analytically. In the semi-analytical approach [1], which is most commonly used, some of the derivatives involved are calculated once again using the finite difference technique. This can be expensive and often inaccurate. Therefore, efforts are currently being made in developing completely analytical approaches for DSA.

Considerable advances have been made recently in the development of DSA of nonlinear structures. Comprehensive reviews of the literature were given by Haftka and Adelman [2] and Kamat [3]. Several theories have been proposed based on continuum formulation. Tsay et al. [4] presented a direct differentiation approach and an adjoint variable approach for DSA of structures with geometric and material nonlinearities. The shape and nonshape design problems were unified using the reference volume concept. Vidal et al. [5] discussed the DSA of history dependent problems. Lee et al. [6] developed DSA of structural systems with elastoplastic material behavior using the continuum

formulation. The above studies were limited to isotropic materials. Since composites are increasingly becoming popular in structural applications, recently research in DSA was extended to composite structures by Chattopadhyay and Guo [7] and a nonlinear DSA approach was presented for composites undergoing elastoplastic deformations. A rate (time-independent) model was employed to account for the plastic material behavior. A higher order approximation of the integration of the rate constitutive equations was proposed in the plastic range. The direct differentiation approach was combined with the reference volume concept. A design partial differentiation approach of the rate constitutive equations was developed and used in the DDA procedure.

The continuum approach is difficult to implement in practical engineering applications. Therefore, a discrete approach is often more practical where the structure is discretized using finite elements and the resulting discretized set of governing equations are used in the DSA. Lee et al. [6] developed a discrete approach by adopting the DDA approach into a finite element procedure. In the numerical implementation, the semi-analytical method was employed and an incremental procedure which often requires iterations was used to solve for the system sensitivities.

In this paper, the continuum DDA approach proposed by Chattopadhyay and Guo [7] is adopted within a finite-element procedure to develop design sensitivities of composite plates undergoing buckling and postbuckling. The reference volume concept is used to unify shape and nonshape design variables. A linear elastic material model and nonlinear strain-displacement relations are used in the present work. This finite element-based procedure of DSA yields a set of linear algebraic equations of sensitivity derivatives of response variables with respect to design variables. The sensitivity derivatives are obtained directly from the current load and responses by solving the set of linear equations.

2. DESIGN SENSITIVITY ANALYSIS OF POSTBUCKLING

The postbuckling analysis of laminated plates, using the classical theory, is outlined below. This is followed by the development of the DSA procedure for postbuckling responses.

2.1. Virtual Work Equations

Figure 1 shows the force analysis of a plate. In this figure N_x, N_y and N_{xy} represent in-plane stress resultants, M_x, M_y and M_{xy} represent stress moments and Q_x and Q_y denote shear resultants. The quantities $\overline{N}_x$ and $\overline{N}_y$ represent boundary in-plane stress resultants, $\overline{M}_x$ and $\overline{M}_y$ represent boundary stress moments and $\overline{Q}$ represent boundary shear resultant. The virtual work equation for the postbuckling of the plate is convenient for the development of a finite element procedure and is written as follows [10].

$$\int_\Omega \left(\frac{\partial \delta u}{\partial x} N_x + \frac{\partial \delta u}{\partial y} N_{xy} \right) dxdy = \int_\Gamma \overline{N}_x \delta u ds$$

$$\int_\Omega \left(\frac{\partial \delta v}{\partial x} N_{xy} + \frac{\partial \delta v}{\partial y} N_y \right) dxdy = \int_\Gamma \overline{N}_y \delta v ds \qquad (1)$$
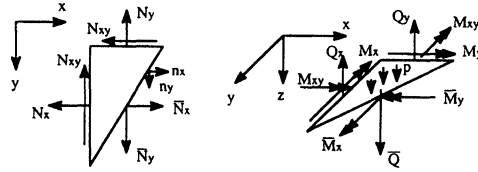
Figure 1 Force analysis of a plate.

$$\int_\Omega \left[\frac{\partial^2 \delta w}{\partial x^2} M_x + \frac{\partial^2 \delta w}{\partial y^2} M_y + 2 \frac{\partial^2 \delta w}{\partial y^2} M_{xy} + \delta w (N_x \frac{\partial^2 w}{\partial x^2} + N_y \frac{\partial^2 w}{\partial y^2} + 2N_{xy} \frac{\partial^2 w}{\partial x \partial y}) \right] dxdy$$

$$= \int_\Gamma \left[\left(\frac{\partial \delta w}{\partial x} \overline{M}_x + \frac{\partial \delta w}{\partial y} \overline{M}_y \right) - \delta w \overline{Q} \right] ds$$

where δu, δv, and δw represent the variations of the mid-plane displacements u, v and w, respectively, Ω represents the domain of the plate and Γ represents the boundary of the plate.

2.2. Finite-Element Model

In an arbitrarily element e with domain Ω^e and boundary Γ^e, the mid-plane displacements u, v and w are approximated as follows.

$$u = \sum_{k=1}^{m} u_k^e \psi_k (\xi, \eta)$$

$$v = \sum_{k=1}^{m} v_k^e \psi_k (\xi, \eta) \qquad (2)$$

$$w = \sum_{k=1}^{n} \Delta_k^e \phi_k (\xi, \eta)$$

where u_k^e and v_k^e denote the nodal values of u and v, respectively and Δ_k^e denote w and its derivatives with respect to x and y. The quantities ξ and η denote the natural coordinates ($-1 \leq \xi, \eta \leq 1$), $\psi_k(\xi, \eta)$ denote the Lagrange interpolation functions and $\phi_k(\xi, \eta)$ denote the Hermite interpolation functions.

Substituting Eqns. (2) for u, v and w into Eqns. (1) and using $\delta u = \psi_i$, $\delta v = \psi_i$ and $\delta w = \phi_j$ yields the finite element representation of the governing equation for element e as follows.

$$\int_{\Omega^e} R_i \, dxdy = \int_{\Gamma^e} \overline{N}_x \psi_i \, ds \quad (i = 1, ..., m)$$

$$\int_{\Omega^e} S_i \, dxdy = \int_{\Gamma^e} \overline{N}_y \psi_i \, ds \quad (i = 1, ..., m) \tag{3}$$

$$\int_{\Omega^e} T_j \, dxdy = - \int_{\Gamma^e} [(\frac{\partial \phi_j}{\partial x} \overline{M}_x + \frac{\partial \phi_j}{\partial y} \overline{M}_y) - \phi_j \overline{Q}] \, ds \quad (j = 1, ..., n)$$

The expressions for the quantities R_i, S_i and T_j are listed in the Appendix A.

Assembly and imposition of the boundary conditions yields a set of asymmetric and nonlinear equations of the global nodal displacement vector. The set of equations can be written in matrix form as follows.

$$\mathbf{KU} = \mathbf{F} \tag{4}$$

where $\mathbf{U}$ represents the global nodal displacement vector and $\mathbf{K}$ represents the global stiffness matrix which is a function of $\mathbf{U}$. The quantity $\mathbf{F}$ represents the external force vector. Several approaches can be used to solve the nonlinear equations [8], [10], [11]. In this paper, a direct iterative method is used.

Let $\mathbf{q}$ be the design variable vector. Its components can include the plate geometry or the material properties. Since $\mathbf{q}$ may include both nondomain (e.g., plate thickness) and domain design variables (e.g., plate width and length), the reference volume concept is used. Using this concept, a reference volume with domain $'\Omega$ and boundary $'\Gamma$ is defined which remains fixed during the design procedure. Let $'\mathbf{q}$ represent the design variable vector corresponding to the reference domain. The actual domain coordinates x and y are related to the reference domain coordinates $'x$ and $'y$ through the following transformation.

$$x = x \, (\mathbf{q}, \, '\mathbf{q}, \, 'x, \, 'y)$$

$$y = y \, (\mathbf{q}, \, '\mathbf{q}, \, 'x, \, 'y) \tag{5}$$

Equations (5) transform the domain Ω with boundary Γ into the reference domain $'\Omega$ with boundary $'\Gamma$.

The area Jacobian $'J$ and the line Jacobian $'J_\Gamma$ are calculated, respectively, as follows.

$$'J = {'J} \, (\mathbf{q}, '\mathbf{q}, 'x, 'y) = det \begin{bmatrix} \dfrac{\partial x}{\partial 'x} & \dfrac{\partial y}{\partial 'x} \\ \dfrac{\partial x}{\partial 'y} & \dfrac{\partial y}{\partial 'y} \end{bmatrix} \tag{6}$$

and

$$'J_\Gamma = \sqrt{(\frac{\partial x}{\partial 'x} \cos \alpha + \frac{\partial x}{\partial 'y} \sin \alpha)^2 + (\frac{\partial y}{\partial 'x} \cos \alpha + \frac{\partial y}{\partial 'y} \sin \alpha)^2} \tag{7}$$

where α is the directional angle of the boundary tangent.

Using Eqs. (6) and (7), the element e with domain Ω^e and boundary Γ^e is transformed to element e with domain $^r\Omega^e$ and boundary $^r\Gamma^e$ in the reference volume. Equations (3) are now expressed in the reference domain as follows.

$$\int_{^r\Omega^e} R_i \, {}^rJ \, d^rx \, d^ry = \int_{^r\Gamma^e} \bar{N}_x \psi_i \, {}^rJ_\Gamma \, dl \qquad (i = 1, ..., m)$$

$$\int_{^r\Omega^e} S_i \, {}^rJ \, d^rx \, d^ry = \int_{^r\Gamma^e} \bar{N}_y \psi_i \, {}^rJ_\Gamma \, dl \qquad (i = 1, ..., m) \tag{8}$$

$$\int_{^r\Omega^e} T_j \, {}^rJ \, d^rx \, d^ry = - \int_{^r\Gamma^e} [(\frac{\partial \phi_j}{\partial x} \bar{M}_x + \frac{\partial \phi_j}{\partial y} \bar{M}_y) - \phi_j \bar{Q}] \, {}^rJ_\Gamma dl \qquad (j = 1, ..., n)$$

Taking the derivatives of Eqs. (8), with respect to the design variable vector $\mathbf{q}$, the governing equations of the design sensitivity are written as follows.

$$\int_{^r\Omega^e} (\frac{dR_i}{d\mathbf{q}} \, {}^rJ + R_i \frac{d^rJ}{d\mathbf{q}}) \, d^rx \, d^ry = \int_{^r\Gamma^e} \psi_i \, (\frac{d\bar{N}_x}{d\mathbf{q}} J_\Gamma + \bar{N}_x \frac{d^rJ_\Gamma}{d\mathbf{q}}) \, dl \qquad (j = 1, ..., m)$$

$$\int_{^r\Omega^e} (\frac{dS_i}{d\mathbf{q}} \, {}^rJ + S_i \frac{d^rJ}{d\mathbf{q}}) \, d^rx \, d^ry = \int_{^r\Gamma^e} \psi_i \, (\frac{d\bar{N}_y}{d\mathbf{q}} J_\Gamma + \bar{N}_y \frac{d^rJ_\Gamma}{d\mathbf{q}}) \, dl \qquad (j = 1, ..., m) \tag{9}$$

$$\int_{^r\Omega^e} (\frac{dT_j}{d\mathbf{q}} {}^rJ + T_j \frac{d^rJ}{d\mathbf{q}}) \, d^rx \, d^ry = - \int_{^r\Gamma^e} \{ [(\frac{\partial \phi_j}{\partial x} \bar{M}_x + \frac{\partial \phi_j}{\partial y} \bar{M}_y) - \phi_j \bar{Q}] \frac{d^rJ_\Gamma}{d\mathbf{q}} +$$

$$[\frac{d}{d\mathbf{q}} (\frac{\partial \phi_j}{\partial x}) \bar{M}_x + \frac{\partial \phi_j}{\partial x} \frac{d\bar{M}_x}{d\mathbf{q}} + \frac{d}{d\mathbf{q}} (\frac{\partial \phi_j}{\partial y}) \bar{M}_y + \frac{\partial \phi_j}{\partial y} \frac{d\bar{M}_y}{d\mathbf{q}} - \phi_j \frac{d\bar{Q}}{d\mathbf{q}}]^rJ_\Gamma \} \, dl \qquad (j = 1, ..., n)$$

It must be noted that in the above equations, the quantities ψ_i and ϕ_j are independent of the design variables since they are only functions of the natural coordinates. Further, according to the concept of equilibrium of secondary variables of element boundaries [8], the assembly of the elements either eliminates the secondary variables ($\bar{N}_x$, $\bar{N}_y$, $\bar{M}_x$, $\bar{M}_y$, and $\bar{Q}$) and their sensitivities ($d\bar{N}_x/d\mathbf{q}$, $d\bar{N}_y/d\mathbf{q}$, $d\bar{M}_x/d\mathbf{q}$, $d\bar{M}_y/d\mathbf{q}$ and $d\bar{Q}/d\mathbf{q}$) or assigns them prescribed values. The expression for the quantities $dR_i/d\mathbf{q}$, $dS_i/d\mathbf{q}$ and $dT_j/d\mathbf{q}$ are listed in Appendix B. An important observation is that the quantities $dR_i/d\mathbf{q}$, $dS_i/d\mathbf{q}$ and $dT_j/d\mathbf{q}$ are linear functions of the response sensitivities $du^e/d\mathbf{q}$, $dv^e/d\mathbf{q}$ and $d\Delta_j^e/d\mathbf{q}$. Assembly techniques, similar to finite element procedure, are employed to obtain the global stiffness sensitivity matrix and the global force sensitivity vector. Next, the boundary conditions are imposed. Finally, the finite element sensitivity equations are written symbolically as follows.

$$\tilde{\mathbf{K}} \frac{d\mathbf{U}}{d\mathbf{q}} = \tilde{\mathbf{F}} \tag{10}$$

where $d\mathbf{U}/d\mathbf{q}$ represents the global nodal displacement sensitivity matrix and $\tilde{\mathbf{K}}$ represents the generalized global stiffness sensitivity matrix which consists of the known functions

of the global nodal displacement vector $\mathbf{U}$. The quantity $\tilde{\mathbf{F}}$ represents the generalized global external force sensitivity vector. Note that once the displacement responses are obtained from the finite element analysis, the quantities $\tilde{\mathbf{K}}$ and $\tilde{\mathbf{F}}$ can be determined. Equations (10) represent a set of linear algebraic equations in $d\mathbf{U}/d\mathbf{q}$, which are easy to solve.

Once the nodal displacement sensitivities are obtained, the stress sensitivities are calculated by direct differentiation of the stress-strain relations and the strain-displacement relations.

3. RESULTS AND DISCUSSIONS

In this section, numerical results of the developed finite element based DSA procedure are presented for both isotropic and composite plates undergoing buckling and postbuckling. A plate of length a, width b and constant thickness h is used (Fig. 2). The plate is assumed to be simply supported on its edges and subjected to in-plane compressive force per unit length, $\bar{N}_x$, in the x direction (Fig. 2). Since the structure and the applied loads are symmetric, only the part of the plate in the quadrant I is analyzed. A four-node noncomforming rectangular element is used in the finite element implementation. A 4×4 mesh and a 8×8 mesh are used in quadrant I in the numerical computations.

To demonstrate the procedure developed, results are presented for isotropic, orthotropic and a cross-ply laminated plates. The mid-plane deflections (w) of the plates are computed at the centers of the plates and the surface stresses σ_1 (in the principal material direction) are computed at the reduced Gauss points which are closest to the plate centers. The sensitivity derivatives of both w and σ_1 with respect to the domain design variable a (plate length) and the nondomain design variable h (plate thickness) are presented. A value of $a = b = 10$in and $h = 1$in is used for the plates. The materials properties are as follows.

Isotropic: E = 1.0 × 10^7 psi, G = 0.4 × 10^7 psi, ν = 0.25

Gl/Ep: E_L/E_T = 3, G_{LT}/E_T = 0.5, ν_{LT} = 0.25

Gr/Ep: E_L/E_T = 40, G_{LT}/E_T = 0.5, ν_{LT} = 0.25
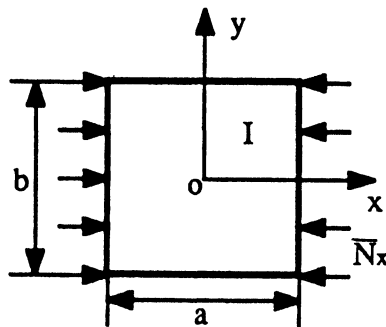

Figure 2 Simply supported rectangular plate subjected to in-plane force, $\bar{N}_x$, with constant thickness h.

where E, G and ν represent, respectively, the Young's modulus, the shear modulus and the Poisson's ratio of the materials. The subscripts L and T denote longitudinal and transverse direction, respectively.

To validate the finite-element-based postbuckling analysis procedure, the responses are compared with exact solutions which were obtained by double Fourier series and generalized double Fourier series [12]. These series solutions are said to be exact in the sense that an infinite set of nonlinear set of nonlinear algebraic equations can be truncated to obtain any desired degree of accuracy. The variations of the load $\bar{N}_x$, normalized with respect to the critical buckling load N_{cr}, are plotted against normalized mid-plane displacement (w/h) in Fig. 3 for the isotropic plate and in Fig. 4 for the Gl/Ep singlelayered orthotropic plate. Figure 5 presents the load-deflection curve of a $(0/90)_4$ Gr/Ep laminated plate with the load, $\bar{N}_x$, normalized by the factor $b^2/E_T h^3$. These results show exact match up to primary buckling. In the postbuckling region, the results of the 8×8 mesh show better agreement with the series solutions than those of the 4×4 mesh.

Figures 6–19 present comparisons of the central deflection sensitivities and stress sensitivities obtained from the finite element sensitivity (FES) analysis procedure with those obtained using the finite difference sensitivity (FDS) analysis procedure using an incremental step of 0.0001. Both domain (length, a) and nondomain (thickness, h) design variables are used.

Figures 6 presents the comparison of the sensitivities of the central deflection with respect to the plate length (a) for the isotropic plate during the complete loading process. Theoretically, the sensitivities of the central deflection with respect to any of the design variables must be zero in the prebuckling stage since the central deflection itself is zero in this region. This is verified by the developed FES procedure in both 4×4 and 8×8 mesh results. However, as shown in Fig. 6, the results of the FDS procedure show serious error by producing nonzero values in the 4×4 mesh case. Obviously, the 4×4 mesh is inadequate for the FDS analysis. Therefore, in the subsequent discussions, only the 8×8 mesh results are presented. For clarity, the postbuckling region alone is presented in Fig.
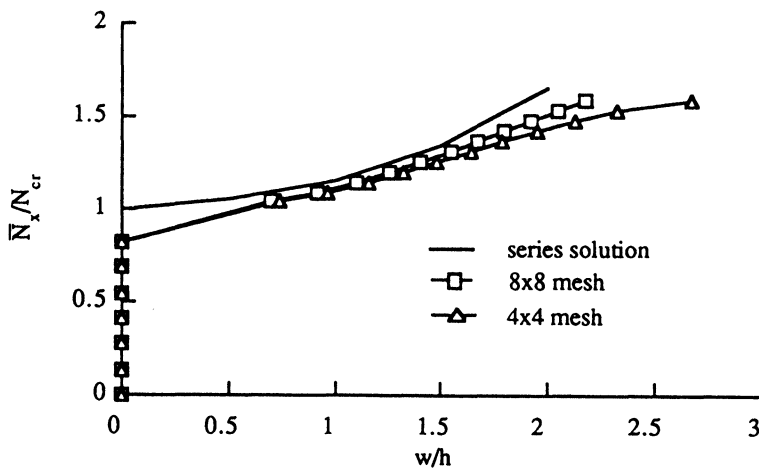

Figure 3   Comparison of postbuckling responses of isotropic plate; $N_{cr} = 3.656 \times 10^5$ lb/in.
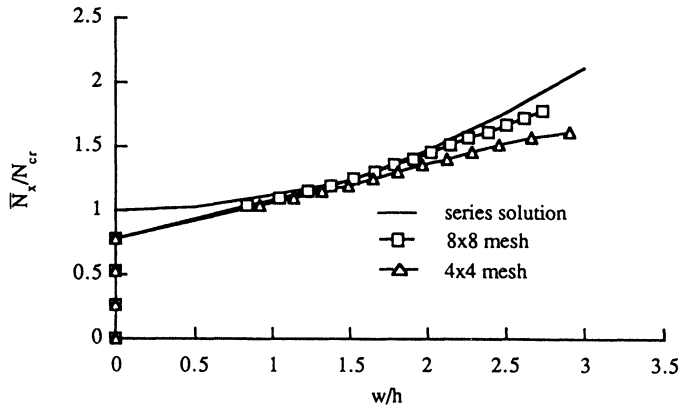
Figure 4 Comparison of postbuckling responses of Gl/Ep single layered orthotropic plate; $N_{cr} = 1.918 \times 10^5$ lb/in.
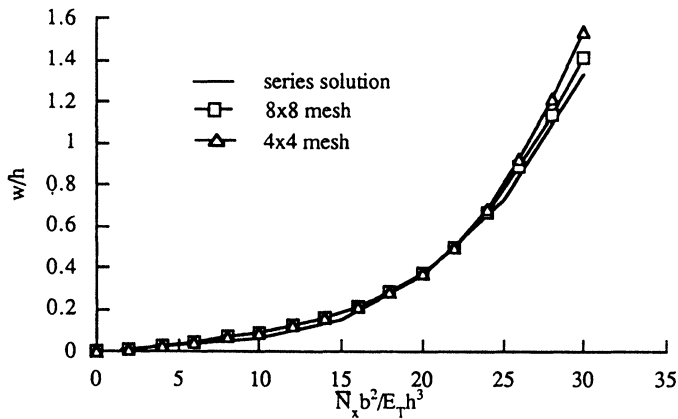

Figure 5 Comparison of central deflection (w/h); $(0/90)_4$Gr/Ep laminated plate.
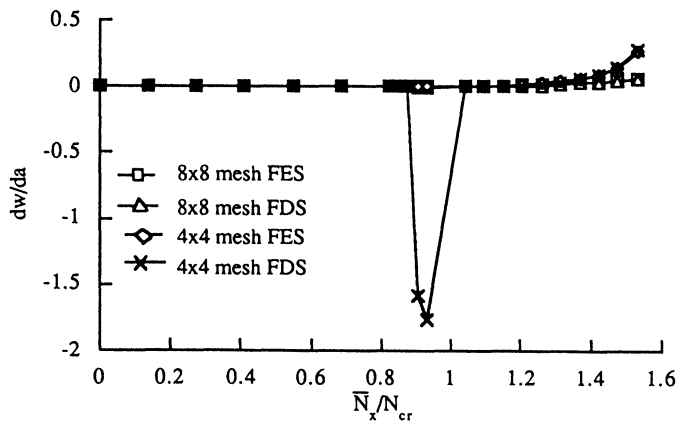

Figure 6 Comparison of sensitivities of central deflection (dw/da); isotropic plate; complete loading; $N_{cr} = 3.656 \times 10^5$ lb/in.
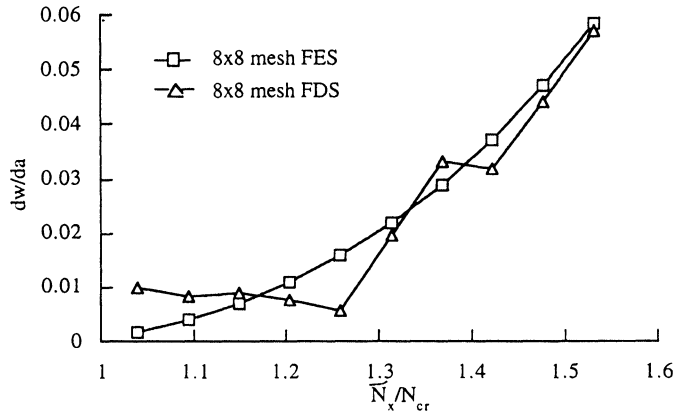
Figure 7 Comparison of postcritical sensitivities of central deflection (dw/da); isotropic plate; $N_{cr} = 3.656 \times 10^5$ lb/in.

7. In this range the results of the FES are better than those of the FDS. The fluctuations observed in the FDS results point to the instability of the technique.

Figure 8 presents the comparison of the sensitivities of the central deflection with respect to the plate thickness (h) for the isotropic plate during the complete loading process. The results agree very well. However, it can be seen that the sensitivity at the buckling load is discontinuous. This can be explained as follows. At critical buckling, the value of the deflection changes from zero to a nonzero value which results in a big jump in the sensitivity.

Figures 9 and 10 present the comparisons of the sensitivities of stress σ_1 (in the principal material direction) with respect to the length (a) and the plate thickness (h), respectively, for the isotropic plate. The results show jump in the sensitivities near the buckling load
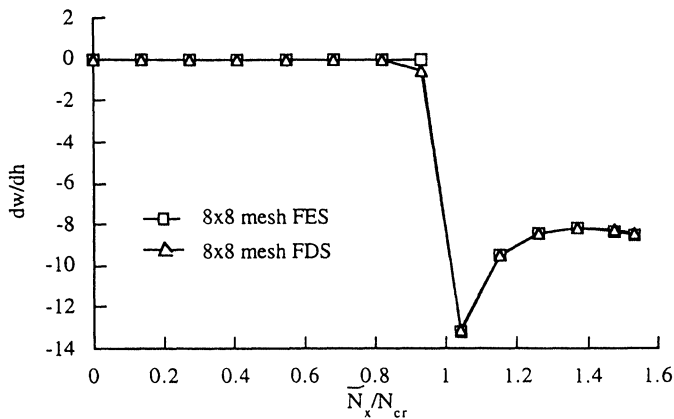

Figure 8 Comparison of sensitivities of central deflection (dw/dh); isotropic plate; complete loading; $N_{cr} = 3.656 \times 10^5$ lb/in.
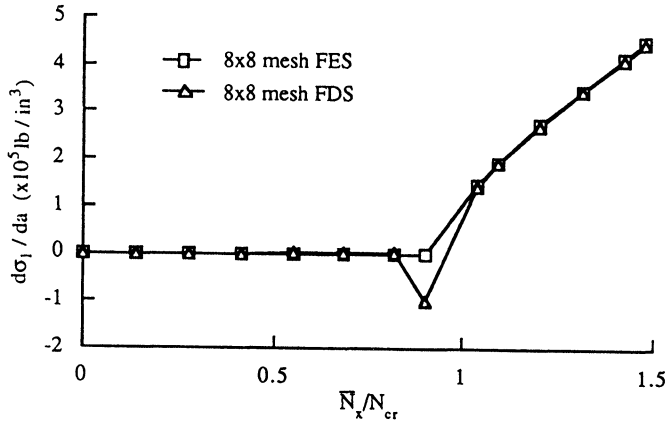
Figure 9 Comparison of stress sensitivities, $(d\sigma_1/da)$; isotropic plate; complete loading; $N_{cr} = 3.656 \times 10^5$ lb/in.

which is a result of the discontinuity of the deflection sensitivity at this point. The results of the FES agree very well with those of the FDS.

Figure 11 presents the comparison of the sensitivities of the central deflection with respect to the plate length (a) for the Gl/Ep single layered orthotropic plate during the complete loading process. Once again, serious error near the buckling load is observed with the FDS results even with 8×8 mesh. Figure 12 presents the postbuckling region only and shows that the results of the FES agree very well with those of the FDS. The comparison of the sensitivities of the central deflection with respect to the thickness (h) for the orthotropic plate during the complete loading process are presented in Figure 13. Once again, the discontinuity of the sensitivity at the buckling point is observed using both techniques. However, for the most part, good agreement is seen between the results of the FES and the FDS.

Figures 14 and 15 present the comparisons of the sensitivities of stress σ_1 with respect to the plate length (a) and the plate thickness (h), respectively, for the orthotropic plate during the complete loading. Once again the sensitivities near the buckling points are
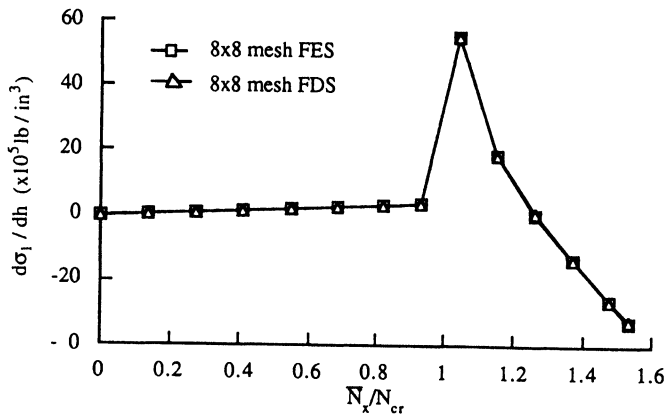

Figure 10 Comparison of stress sensitivities $(d\sigma_1/dh)$; isotropic plate; complete loading; $N_{cr} = 3.656 \times 10^5$ lb/in.
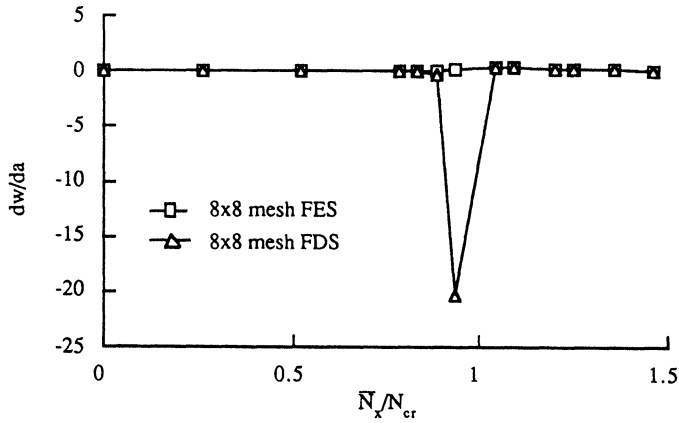
Figure 11 Comparison of sensitivities of central deflection (dw/da); Gl/Ep single layered orthotropic plate; complete loading; $N_{cr} = 1.918 \times 10^5$ lb/in.
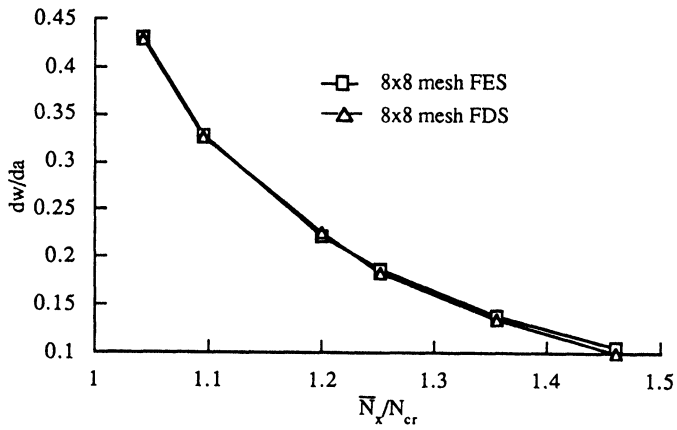

Figure 12 Comparison of postcritical sensitivities of central deflection (dw/da); Gl/Ep single-layered orthotropic plate; $N_{cr} = 1.918 \times 10^5$ lb/in.
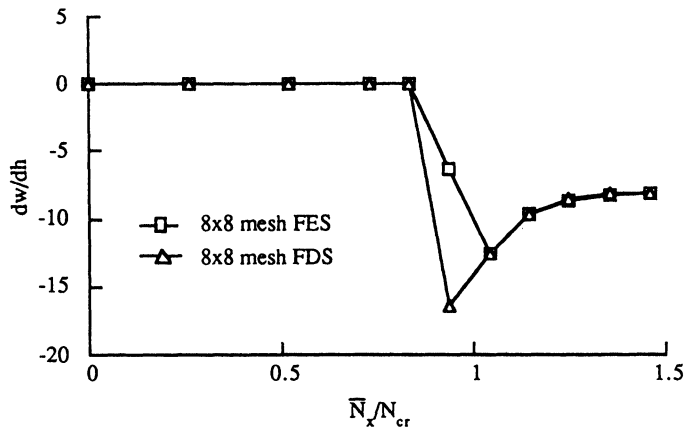

Figure 13 Comparison of sensitivities of central deflection (dw/dh); Gl/Ep single layered orthotropic plate; complete loading; $N_{cr} = 1.918 \times 10^5$ lb/in.
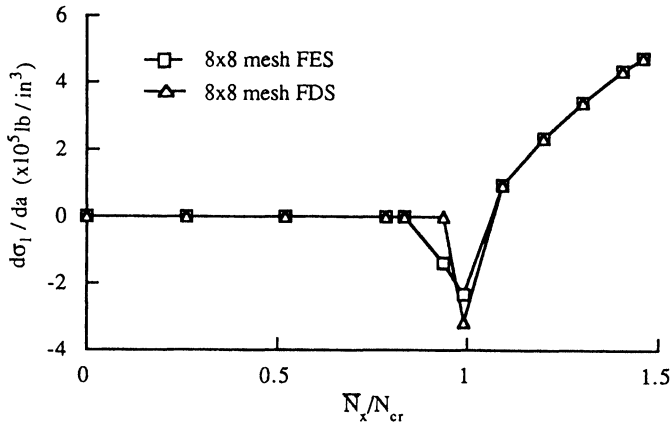
Figure 14 Comparison of stress sensitivities $(d\sigma_1/da)$; Gl/Ep single layered orthotropic plate; complete loading; $N_{cr} = 1.918 \times 10^5$ lb/in.

discontinuous in both cases. However, the agreements are excellent between the FES and the FDS approach over the remaining region.

Figures 16 and 17 present the comparisons of the central deflection sensitivities with respect to the plate length (a) and the plate thickness (h), respectively, for the $(0/90)_4$ Gr/Ep laminated plate during the complete loading process. Figure 16 shows that the results of the FES procedure agree very well with those obtained using the FDS for moderate values of $\bar{N}_x$. At higher values of $\bar{N}_x$, the results of the FDS deviate from those of the FES. This can be explained as follows. For higher values of the load, the accuracy of the approximations deteriorates and this effect becomes more pronounced when finite difference technique is used. Figure 17 shows excellent agreement of the displacement sensitivities, with respect to the nondomain design variable (h), between the FES and the FDS procedures.
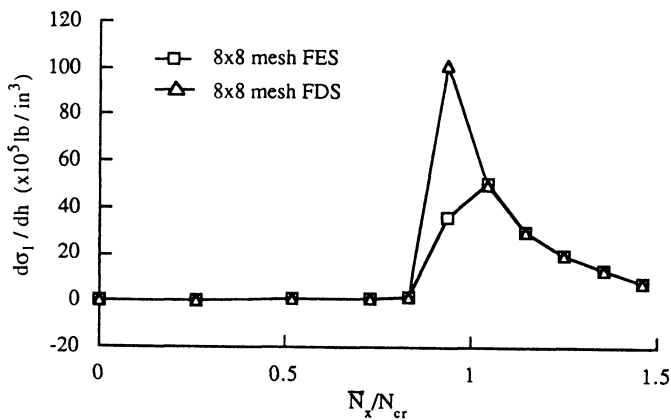

Figure 15 Comparison of stress sensitivities $(d\sigma_1/dh)$; Gl/Ep single layered orthotropic plate; complete loading; $N_{cr} = 1.918 \times 10^5$ lb/in.
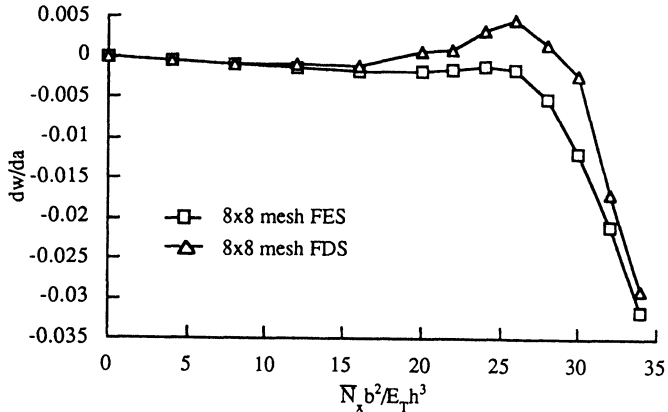
Figure 16 Comparison of sensitivities of central deflection (dw/da); $(0/90)_4$ Gr/Ep laminated plate; complete loading.

Figures 18 and 19 present the comparisons of the sensitivities of stress σ_1 with respect to the plate length (a) and the plate thickness (h), respectively, for the laminated plate during the complete loading process. Excellent agreement is obtained between the results of the FES and those of the FDS.

From the above discussion, the following conclusions can be made. At the buckling point, the sensitivities derivatives are discontinuous for both isotropic and orthotropic plates. For the cross-ply laminated plate, in which there is no critical buckling point, the sensitivities are continuous over the complete loading process.

A comparison of the CPU time is made between the FES and the FDS techniques. Figure 20 presents the comparison of the CPU time for a complete sensitivity analysis which includes calculations of all displacement and stress sensitivities with respect to all three design variables a, b and h (Fig. 2). The load levels corresponding to the isotropic,
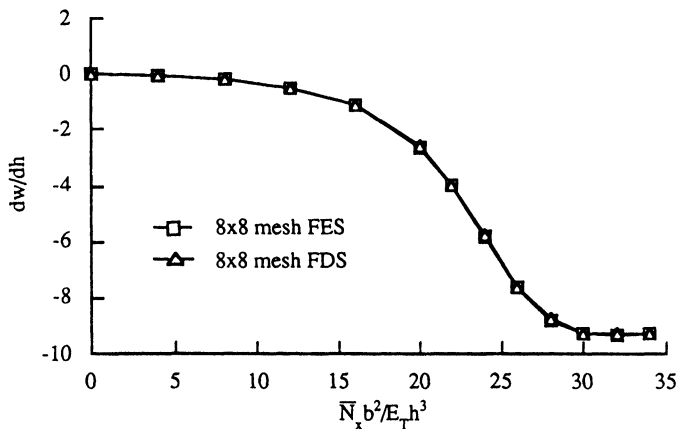

Figure 17 Comparison of sensitivities of central deflection (dw/dh); $(0/90)_4$ Gr/Ep laminated plate; complete loading.
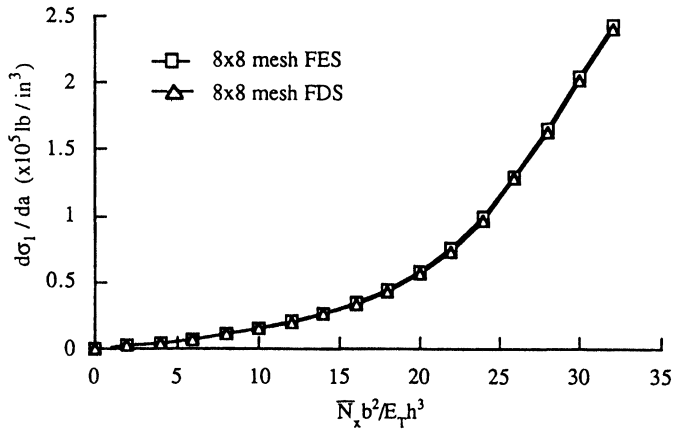
Figure 18 Comparison of stress sensitivities, $(d\sigma_1/da)$, $(0/90)_4$ Gr/Ep laminated plate; complete loading.
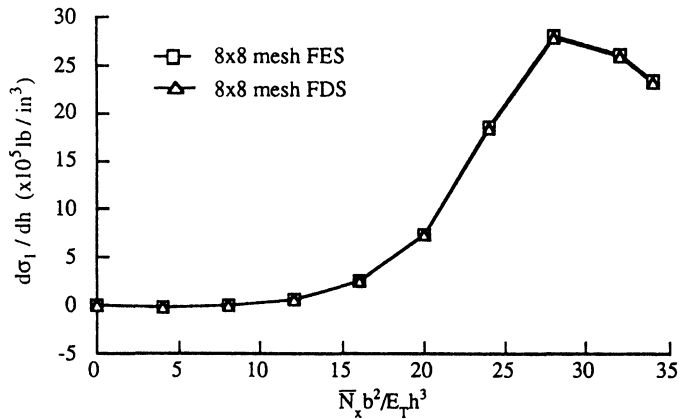

Figure 19 Comparison of stress sensitivities $(d\sigma_1/dh)$ $(0/90)_4$ Gr/Ep laminated plate; complete loading.
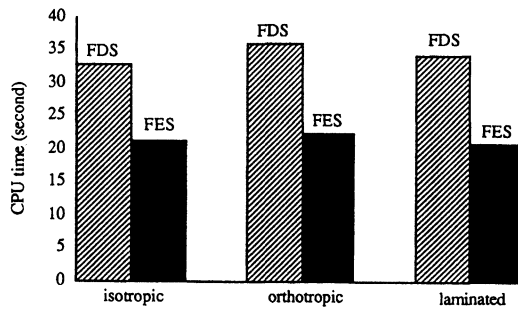

Figure 20 Comparison of CPU time of the FES and FDS.

the orthotropic and the cross-ply laminated plates are $1.3677N_{cr}$, $1.5644N_{cr}$ and $\overline{N}_x = 32E_T h^3/b^2$, respectively. It can be seen that the FES approach saves approximately 40 percent CPU time in all cases.

4. CONCLUSION

A finite-element sensitivity (FES) analysis procedure was developed for the design sensitivity analysis (DSA) of composite plates undergoing buckling and postbuckling. The direct differentiation approach combined with the reference volume concept was applied to address both shape and nonshape design variables. Linear elastic material model and nonlinear geometric relations were adopted. The sensitivity equations obtained from this procedure represent a set of linear algebraic equations in terms of derivatives of the displacement responses with respect to the design variable vector. The sensitivity derivatives were obtained directly from the current load and responses by solving the set of linear equations and no iterations were required. Numerical results were presented for isotropic, orthotropic and $(0/90)_4$ laminated composite plates. Deflection and stress sensitivities were calculated using both domain and nondomain design variables. Results were compared against those obtained using finite difference approach. The following important observations were made from this study.

1) The developed finite-element sensitivity analysis procedure agrees very well with the finite-difference technique except at critical buckling point where discontinuity occurs.
2) The finite-difference sensitivity analysis procedure shows serious accuracy problem in regions close to the buckling load.
3) The approach saves significant CPU time.

Acknowledgements

NOMENCLATURE

a	length of plate
b	width of plate
E_L, E_T	longitudinal and transverse Young's moduli, respectively
F	global external force vector
$\tilde{F}$	generalized global external force sensitivity vector
G	global stability matrix
G^e	element stability matrix
G_{LT}	shear modulus
h	thickness of plate

^rJ	area Jacobian from reference domain to design domain
$^rJ_\Gamma$	line Jacobian from reference domain to design domain
K	global stiffness matrix
K^e	element stiffness matrix
$\tilde{K}$	generalized global stiffness sensitivity matrix
M_x, M_y, M_{xy}	stress moments of plate
$\overline{M}_x, \overline{M}_y$	boundary stress moments of plate
N_x, N_y, N_{xy}	in-plane stress resultants of plate
$\overline{N}_x, \overline{N}_y$	boundary in-plane stress resultants of plate
N_{cr}	critical buckling load of plate
Q_x, Q_y	shear resultants of plate
Q	boundary shear resultant of plate
q	design variable vector of design domain
^rq	design variable vector of reference domain
u	displacement in the x direction
u_i^e	element nodal values of displacement u ($i = 1,\dots, m$)
v	displacement in the y direction
v_i^e	element nodal values of displacement v ($i = 1,\dots, m$)
w	mid-plane deflection of plate
x, y	design domain coordinates
$^rx, {}^ry$	reference domain coordinate vector
Ω	domain of plate
$^r\Omega$	reference domain of plate
Γ	boundary of plate
$^r\Gamma$	reference boundary of plate
ν_{LT}	Poisson's ratio
Δ	global nodal displacement vector
Δ_i^e	element nodal values of w and its derivatives with respect to x and y ($i = 1,\dots, n$)
Ψ_i	Lagrange interpolation functions ($i = 1,\dots, m$)
ϕ_j	Hermite interpolation functions ($j = 1,\dots, n$)
σ_i	stress in principal material direction ($i = 1, 2, 6$)
ξ, η	natural coordinates

References

1. Haftka, R.T., Z. Gurdal, and M.P. Kamat, *Elements of structural optimization*, Kluwer Academic Publishers, 1990.
2. Haftka, R.T. and H.M. Adelman, Recent developments in structural sensitivity analysis, *Structural Optimization*, **1** (1989), 137–151.
3. Kamat, M. (Ed.), *Structural optimization: Status and promise*, AIAA Series on Progress in Astronautics and Aeronautics, American Institute of Aeronautics and Astronautics, Washington, D.C., 1993.
4. Tsay, J.J. and J.S. Arora, Nonlinear structural design sensitivity analysis for path dependent problems. Part 1: General theory, *Computer Methods in Applied Mechanics and Engineering* **81**, (1990), 183–208.
5. Vidal, C.A., H.S. Lee, and R.B. Haber, The consistent tangent operator for design sensitivity analysis of history-dependent response, *Comp. Systems in Engrg.*, **2** (1991), 509–523.
6. Lee, T.H. and J.S. Arora, Numerical implementation of design sensitivity analysis of elastoplastic structures, *Proc. of the 34th AIAA/ASME/ASCE/AHS/ASC Structures, Structural Dynamics, and Materials Conference AIAA/ASME Adaptive Structures Forum*, La Jolla, CA, April 19–22, 1993, pp. 1941–1951.

7. Chattopadhyay, A. and R.J. Guo, Nonlinear structural design sensitivity analysis for composites undergoing elastoplastic deformation, presented at *the Army Research Office Workshop on "Dynamic Response of Composite Structures*, New Orleans, LA, August, 1993. *Mathematical and Computer Modelling* (in press).
8. Reddy, J.N., *An introduction to the finite element method*, McGraw-Hill, New York, 1993.
9. Timoshenko, S.P., and J.M., Gere, *Theory of elastic stability*, McGraw-Hill, New York, 1961.
10. Ochoa, O.O, and J.N. Reddy, *Finite element analysis of composite laminates*, Kluwer Academic Publishers, Boston, 1992.
11. Zienkiewicz, O.C., and R.L. Taylor, *The finite element method, Vol. 2: Nonlinear problems*, McGraw-Hill, New York, 1991.
12. Chia, C.Y., *Nonlinear analysis of plates*, McGraw-Hill, New York, 1980.

APPENDIX A

$$R_i = (\frac{\partial \psi_i}{\partial x} A_{11} + \frac{\partial \psi_i}{\partial y} A_{16}) [\sum_{k=1}^{m} u_k^e \frac{\partial \pi_k}{\partial x} + \frac{1}{2} (\sum_{k=1}^{n} \Delta_k^e \frac{\partial \phi_k}{\partial x})^2] + (\frac{\partial \psi_i}{\partial x} A_{12} + \frac{\partial \psi_i}{\partial y} A_{26})$$

$$[\sum_{k=1}^{m} v_k^e \frac{\partial \psi_k}{\partial y} + \frac{1}{2} (\sum_{k=1}^{n} \Delta_k^e \frac{\partial \phi_k}{\partial y})^2] + (\frac{\partial \psi_i}{\partial x} A_{16} + \frac{\partial \psi_i}{\partial y} A_{66})[\sum_{k=1}^{m} u_k^e \frac{\partial \psi_k}{\partial y} +$$

$$\sum_{k=1}^{m} v_k^e \frac{\partial \psi_k}{\partial x} + (\sum_{k=1}^{n} \Delta_k^e \frac{\partial \phi_k}{\partial x})(\sum_{k=1}^{n} \Delta_k^e \frac{\partial \phi_k}{\partial y})] - (\frac{\partial \psi_i}{\partial x} B_{11} + \frac{\partial \psi_i}{\partial y} B_{16})(\sum_{k=1}^{n} \Delta_k^e \frac{\partial^2 \phi_k}{\partial x^2} - \quad (11)$$

$$(\frac{\partial \psi_i}{\partial x} B_{12} + \frac{\partial \psi_i}{\partial y} B_{26})(\sum_{k=1}^{n} \Delta_k^e \frac{\partial^2 \phi_k}{\partial y^2} - 2(\frac{\partial \psi_1}{\partial x} B_{16} + \frac{\partial \psi_i}{\partial y} B_{66})(\sum_{k=1}^{n} \Delta_k^e \frac{\partial^2 \phi_k}{\partial x \partial y})$$

$$S_i = (\frac{\partial \psi_i}{\partial x} A_{16} + \frac{\partial \psi_i}{\partial y} A_{12}) [\sum_{k=1}^{m} u_k^e \frac{\partial \psi_k}{\partial x} + \frac{1}{2} (\sum_{k=1}^{n} \Delta_k^e \frac{\partial \phi_k}{\partial x})^2] + (\frac{\partial \psi_i}{\partial x} A_{26} + \frac{\partial \psi_i}{\partial y} A_{22})$$

$$[\sum_{k=1}^{m} v_k^e \frac{\partial \psi_k}{\partial y} + \frac{1}{2} (\sum_{k=1}^{n} \Delta_k^e \frac{\partial \phi_k}{\partial y})^2] + (\frac{\partial \psi_i}{\partial x} A_{66} + \frac{\partial \psi_i}{\partial y} A_{26}) [\sum_{k=1}^{m} u_k^e \frac{\partial \psi_k}{\partial y} +$$

$$\sum_{k=1}^{m} v_k^e \frac{\partial \psi_k}{\partial x} + (\sum_{k=1}^{n} \Delta_k^e \frac{\partial \phi_k}{\partial x})(\sum_{k=1}^{n} \Delta_k^e \frac{\partial \phi_k}{\partial y})] - (\frac{\partial \psi_i}{\partial x} B_{16} + \frac{\partial \psi_i}{\partial y} B_{12})(\sum_{k=1}^{n} \Delta_k^e \frac{\partial^2 \phi_k}{\partial x^2} - \quad (12)$$

$$(\frac{\partial \psi_i}{\partial x} B_{26} + \frac{\partial \psi_i}{\partial y} B_{22})(\sum_{k=1}^{n} \Delta_k^e \frac{\partial^2 \phi_k}{\partial y^2} - 2(\frac{\partial \psi_1}{\partial x} B_{66} + \frac{\partial \psi_i}{\partial y} B_{26})(\sum_{k=1}^{n} \Delta_k^e \frac{\partial^2 \phi_k}{\partial x \partial y})$$

$$T_i = [\sum_{k=1}^{m} u_k^e \frac{\partial \psi_k}{\partial x} + \frac{1}{2} (\sum_{k=1}^{n} \Delta_k^e \frac{\partial \phi_k}{\partial x})^2]\{\frac{\partial^2 \phi_j}{\partial x^2} B_{11} + \frac{\partial^2 \phi_j}{\partial x^2} B_{12} + 2 \frac{\partial^2 \phi_j}{\partial x \partial y} B_{16} + \phi_j[A_{11} \sum_{k=1}^{n} \Delta_k^e \frac{\partial^2 \phi_k}{\partial x^2}) +$$

$$A_{12} (\sum_{k=1}^{n} \Delta_k^e \frac{\partial^2 \phi_k}{\partial y^2}) + 2A_{16} (\sum_{k=1}^{n} \Delta_k^e \frac{\partial^2 \phi_k}{\partial x \partial y})]\} + [\sum_{k=1}^{m} v_k^e \frac{\partial \psi_k}{\partial x} + \frac{1}{2} (\sum_{k=1}^{n} \Delta_k^e \frac{\partial \phi_k}{\partial y})^2]\{\frac{\partial^2 \phi_j}{\partial x^2} B_{12} +$$

$$\frac{\partial^2 \phi_j}{\partial y^2} B_{22} + 2 \frac{\partial^2 \phi_j}{\partial x \partial y} B_{26} + \phi_j[A_{12} (\sum_{k=1}^{n} \Delta_k^e \frac{\partial^2 \phi_k}{\partial x^2}) + A_{22} (\sum_{k=1}^{n} \Delta_k^e \frac{\partial^2 \phi_k}{\partial y^2}) + 2A_{26} (\sum_{k=1}^{n} \Delta_k^e \frac{\partial^2 \phi_k}{\partial x \partial y})]\} +$$

$$[\sum_{k=1}^{m} u_k^e \frac{\partial \psi_k}{\partial y} + \sum_{k=1}^{m} v_k^e \frac{\partial \psi_k}{\partial y} + (\sum_{k=1}^{n} \Delta_k^e \frac{\partial \phi_k}{\partial x}) (\sum_{k=1}^{n} \Delta_k^e \frac{\partial \phi_k}{\partial y})]\{\frac{\partial^2 \phi_j}{\partial x^2} B_{16} + \frac{\partial^2 \phi_j}{\partial y^2} B_{26} + 2 \frac{\partial^2 \phi_j}{\partial x \partial y} B_{66} + \phi_j$$

$$[A_{16} (\sum_{k=1}^{n} \Delta_k^e \frac{\partial^2 \phi_k}{\partial y^2}) + A_{26} (\sum_{k=1}^{n} \Delta_k^e \frac{\partial^2 \phi_k}{\partial y^2}) + 2A_{66} (\sum_{k=1}^{n} \Delta_k^e \frac{\partial^2 \phi_k}{\partial x \partial y^2})]\} - (\sum_{k=1}^{n} \Delta_k^e \frac{\partial^2 \phi_k}{\partial x^2})\{\frac{\partial^2 \phi_j}{\partial x^2} C_{11} +$$

$$\frac{\partial^2 \phi_j}{\partial y^2} C_{12} + 2 \frac{\partial^2 \phi_j}{\partial x \partial y} C_{16} + \phi_j [B_{11} (\sum_{k=1}^{n} \Delta_k^e \frac{\partial^2 \phi_k}{\partial x^2}) + B_{12} (\sum_{k=1}^{n} \Delta_k^e \frac{\partial^2 \phi_k}{\partial y^2}) + 2B_{16} (\sum_{k=1}^{n} \Delta_k^e \frac{\partial^2 \phi_k}{\partial x \partial y})]\} -$$

$$(\sum_{k=1}^{n} \Delta_k^e \frac{\partial^2 \phi_k}{\partial y^2}) \{\frac{\partial^2 \phi_j}{\partial x^2} C_{12} + \frac{\partial^2 \phi_j}{\partial y^2} C_{22} + 2 \frac{\partial^2 \phi_j}{\partial x \partial y} C_{26} + \phi_j [B_{12} (\sum_{k=1}^{n} \Delta_k^e \frac{\partial^2 \phi_k}{\partial x^2}) + B_{22} (\sum_{k=1}^{n} \Delta_k^e \frac{\partial^2 \phi_k}{\partial y^2}) +$$

$$2B_{26} (\sum_{k=1}^{n} \Delta_k^e \frac{\partial^2 \phi_k}{\partial x \partial y})]\} - (\sum_{k=1}^{n} \Delta_k^e \frac{\partial^2 \phi_k}{\partial x \partial y}) \{\frac{\partial^2 \phi_j}{\partial x^2} C_{16} + \frac{\partial^2 \phi_j}{\partial y^2} C_{26} + 2 \frac{\partial^2 \phi_j}{\partial x \partial y} C_{66} + \tag{13}$$

$$\phi_j [B_{16} (\sum_{k=1}^{n} \Delta_k^e \frac{\partial^2 \phi_k}{\partial x^2}) + B_{26} (\sum_{k=1}^{n} \Delta_k^e \frac{\partial^2 \phi_k}{\partial y^2}) + 2B_{66} (\sum_{k=1}^{n} \Delta_k^e \frac{\partial^2 \phi_k}{\partial x \partial y})]\}$$

where A_{ij}, C_{ij} and B_{ij} (i, j = 1,2,6) are the extensional stiffness, bending stiffness and bending−extensional coupling stiffness of the plate, respectively.

APPENDIX B

$$\frac{dR_i}{d\mathbf{q}} = [\frac{d}{d\mathbf{q}} (\frac{\partial \psi_i}{\partial x}) A_{11} + \frac{\partial \psi_i}{\partial x} \frac{dA_{11}}{d\mathbf{q}} + \frac{d}{d\mathbf{q}} (\frac{\partial \psi_i}{\partial y}) A_{16} + \frac{\partial \psi_i}{\partial y} \frac{dA_{16}}{d\mathbf{q}}]$$

$$[\sum_{k=1}^{m} [\frac{du_k^e}{d\mathbf{q}} \frac{\partial \psi_k}{\partial x} + u_k^e \frac{d}{d\mathbf{q}} (\frac{\partial \psi_k}{\partial x})] + \sum_{k=1}^{n} \Delta_k^e \frac{\partial \phi_k}{\partial x} \sum_{k=1}^{n} [\frac{d\Delta_k^e}{d\mathbf{q}} \frac{\partial \phi_k}{\partial x} + \Delta_k^e \frac{d}{d\mathbf{q}} (\frac{\partial \phi_k}{\partial x})]\} +$$

$$[\frac{d}{d\mathbf{q}} (\frac{\partial \psi_i}{\partial x}) A_{12} + \frac{\partial \psi_i}{\partial x} \frac{dA_{12}}{d\mathbf{q}} + \frac{d}{d\mathbf{q}} (\frac{\partial \psi_i}{\partial y}) A_{26} + \frac{\partial \psi_i}{\partial y} \frac{dA_{26}}{d\mathbf{q}}]$$

$$\{\sum_{k=1}^{m} [\frac{dv_k^e}{d\mathbf{q}} \frac{\partial \psi_k}{\partial y} + v_k^e \frac{d}{d\mathbf{q}} (\frac{\partial \psi_k}{\partial y})] + (\sum_{k=1}^{n} \Delta_k^e \frac{\partial \phi_k}{\partial y}) \sum_{k=1}^{n} [\frac{d\Delta_k^e}{d\mathbf{q}} \frac{\partial \phi_k}{\partial y} + \Delta_k^e \frac{d}{d\mathbf{q}} (\frac{\partial \phi_k}{\partial y})]\} +$$

$$[\frac{d}{d\mathbf{q}} (\frac{\partial \psi_i}{\partial x}) A_{16} + \frac{\partial \psi_i}{\partial x} \frac{dA_{16}}{d\mathbf{q}} + \frac{d}{d\mathbf{q}} (\frac{\partial \psi_i}{\partial y}) A_{66} + \frac{\partial \psi_i}{\partial y} \frac{dA_{66}}{d\mathbf{q}}]$$

$$\{\sum_{k=1}^{m} [\frac{du_k^e}{d\mathbf{q}} \frac{\partial \psi_k}{\partial y} + u_k^e \frac{d}{d\mathbf{q}} (\frac{\partial \psi_k}{\partial y})] + \sum_{k=1}^{m} [\frac{dv_k^e}{d\mathbf{q}} \frac{\partial \psi_k}{\partial x} + v_k^e \frac{d}{d\mathbf{q}} (\frac{\partial \psi_k}{\partial x})] +$$

$$[\sum_{k=1}^{n} (\frac{d\Delta_k^e}{d\mathbf{q}} \frac{\partial \phi_k}{\partial x} + \Delta_k^e \frac{d}{d\mathbf{q}} (\frac{\partial \phi_k}{\partial x})) (\sum_{k=1}^{n} \Delta_k^e \frac{\partial \phi_k}{\partial y}) + (\sum_{k=1}^{n} \Delta_k^e \frac{\partial \phi_k}{\partial x}) \sum_{k=1}^{n} (\frac{d\Delta_k^e}{d\mathbf{q}} \frac{\partial \phi_k}{\partial y} +$$

$$\Delta_k^e \frac{d}{d\mathbf{q}}(\frac{\partial\phi_k}{\partial y}))]\} - [\frac{d}{d\mathbf{q}}(\frac{\partial\psi_i}{\partial x})B_{11} + \frac{\partial\psi_i}{\partial x}\frac{dB_{11}}{d\mathbf{q}} + \frac{d}{d\mathbf{q}}(\frac{\partial\psi_i}{\partial y})B_{16} + \frac{\partial\psi_i}{\partial y}\frac{dB_{16}}{d\mathbf{q}}]\sum_{k=1}^{n}[\frac{d\Delta_k^e}{d\mathbf{q}}\frac{\partial^2\phi_k}{\partial x^2} +$$

$$\Delta_k^e \frac{d}{d\mathbf{q}}(\frac{\partial^2\phi_k}{\partial x^2})] - \frac{d}{d\mathbf{q}}(\frac{\partial\psi_i}{\partial x})B_{12} + \frac{\partial\psi_i}{\partial x}\frac{dB_{12}}{d\mathbf{q}} + \frac{d}{d\mathbf{q}}(\frac{\partial\psi_i}{\partial y})B_{26} + \frac{\partial\psi_i}{\partial y}\frac{dB_{26}}{d\mathbf{q}}]\sum_{k=1}^{n}[\frac{d\Delta_k^e}{d\mathbf{q}}\frac{\partial^2\phi_k}{\partial y^2} +$$

$$\Delta_k^e \frac{d}{d\mathbf{q}}(\frac{\partial^2\phi_k}{\partial y^2})] -2[\frac{d}{d\mathbf{q}}(\frac{\partial\psi_i}{\partial x})B_{16} + \frac{\partial\psi_i}{\partial x}\frac{dB_{16}}{d\mathbf{q}} + \frac{d}{d\mathbf{q}}(\frac{\partial\psi_i}{\partial y})B_{66} + \frac{\partial\psi_i}{\partial y}\frac{dB_{66}}{d\mathbf{q}}]\sum_{k=1}^{n}[\frac{d\Delta_k^e}{d\mathbf{q}}\frac{\partial^2\phi_k}{\partial x\partial y} +$$

$$\Delta_k^e \frac{d}{d\mathbf{q}}(\frac{\partial^2\phi_k}{\partial x\partial y})] \tag{14}$$

The quantities $\frac{dS_i}{d\mathbf{q}}$ and $\frac{dT_i}{d\mathbf{q}}$ can be obtained similarly. The quantities $\frac{d}{d\mathbf{q}}(\frac{\partial\psi_k}{\partial x})$,

$\frac{d}{d\mathbf{q}}(\frac{\partial\psi_k}{\partial y})$, $\frac{d}{d\mathbf{q}}(\frac{\partial\phi_k}{\partial x})$, $\frac{d}{d\mathbf{q}}(\frac{\partial\phi_k}{\partial y})$, $\frac{d}{d\mathbf{q}}(\frac{\partial^2\phi_k}{\partial x^2})$, $\frac{d}{d\mathbf{q}}(\frac{\partial^2\phi_k}{\partial y^2})$ and $\frac{d}{d\mathbf{q}}(\frac{\partial^2\phi_k}{\partial x\partial y})$ are calculated as

follows. The transformation between element coordinates (x,y) and natural coordinates (ξ,η) is written as follows (the superscript e is omitted for brevity).

$$x = \sum_{i=1}^{m} x_i \psi_i(\xi,\eta), \quad y = \sum_{i=1}^{m} y_i\psi_i(\xi,\eta) \tag{15}$$

From Eqn. (15), the following expressions can be obtained.

$$\frac{d}{d\mathbf{q}}(\frac{\partial x}{\partial\xi}) = \sum_{i=1}^{m}\frac{dx_i}{d\mathbf{q}}\frac{\partial\psi_i}{\partial\xi}, \quad \frac{d}{d\mathbf{q}}(\frac{\partial x}{\partial\eta}) = \sum_{i=1}^{m}\frac{dx_i}{d\mathbf{q}}\frac{\partial\psi_i}{\partial\eta}$$

$$\frac{d}{d\mathbf{q}}(\frac{\partial y}{\partial\xi}) = \sum_{i=1}^{m}\frac{dy_i}{d\mathbf{q}}\frac{\partial\psi_i}{\partial\xi}, \quad \frac{d}{d\mathbf{q}}(\frac{\partial y}{\partial\xi}) = \sum_{i=1}^{m}\frac{dy_i}{d\mathbf{q}}\frac{\partial\psi_i}{\partial\xi}$$

$$\frac{d}{d\mathbf{q}}(\frac{\partial^2 x}{\partial\xi^2}) = \sum_{i=1}^{m}\frac{dx_i}{d\mathbf{q}}\frac{\partial^2\psi_i}{\partial\xi^2}, \quad \frac{d}{d\mathbf{q}}(\frac{\partial^2 x}{\partial\eta^2}) = \sum_{i=1}^{m}\frac{dx_i}{d\mathbf{q}}\frac{\partial^2\psi_i}{\partial\eta^2}, \quad \frac{d}{d\mathbf{q}}(\frac{\partial^2 x}{\partial\xi\partial\eta}) = \sum_{i=1}^{m}\frac{dx_i}{d\mathbf{q}}\frac{\partial^2\psi_i}{\partial\xi\partial\eta} \tag{16}$$

$$\frac{d}{d\mathbf{q}}(\frac{\partial^2 y}{\partial\xi^2}) = \sum_{i=1}^{m}\frac{dy_i}{d\mathbf{q}}\frac{\partial^2\psi_i}{\partial\xi^2}, \quad \frac{d}{d\mathbf{q}}(\frac{\partial^2 y}{\partial\eta^2}) = \sum_{i=1}^{m}\frac{dy_i}{d\mathbf{q}}\frac{\partial^2\psi_i}{\partial\eta^2}, \quad \frac{d}{d\mathbf{q}}(\frac{\partial^2 y}{\partial\xi\partial\eta}) = \sum_{i=1}^{m}\frac{dy_i}{d\mathbf{q}}\frac{\partial^2\psi_i}{\partial\xi\partial\eta}$$

Then the quantities $\frac{d}{d\mathbf{q}}(\frac{\partial\psi_k}{\partial x})$, $\frac{d}{d\mathbf{q}}(\frac{\partial\psi_k}{\partial y})$, $\frac{d}{d\mathbf{q}}(\frac{\partial\phi_k}{\partial x})$, $\frac{d}{d\mathbf{q}}(\frac{\partial\phi_k}{\partial y})$, $\frac{d}{d\mathbf{q}}(\frac{\partial^2\phi_k}{\partial x^2})$, $\frac{d}{d\mathbf{q}}(\frac{\partial^2\phi_k}{\partial y^2})$

and $\frac{d}{d\mathbf{q}}(\frac{\partial^2\phi_k}{\partial x\partial y})$ are written as follows.

$$
\left\{
\begin{array}{c}
\dfrac{d}{d\mathbf{q}}\left(\dfrac{\partial \psi_i}{\partial x}\right) \\[2mm]
\dfrac{d}{d\mathbf{q}}\left(\dfrac{\partial \psi_i}{\partial y}\right)
\end{array}
\right\}
=
\begin{bmatrix}
\dfrac{\partial x}{\partial \xi} & \dfrac{\partial y}{\partial \xi} \\[2mm]
\dfrac{\partial x}{\partial \eta} & \dfrac{\partial y}{\partial \eta}
\end{bmatrix}^{-1}
\left\{
\begin{array}{c}
-\dfrac{\partial \psi_i}{\partial x}\dfrac{d}{d\mathbf{q}}\left(\dfrac{\partial x}{\partial \xi}\right) - \dfrac{\partial \psi_i}{\partial y}\dfrac{d}{d\mathbf{q}}\left(\dfrac{\partial y}{\partial \xi}\right) \\[2mm]
-\dfrac{\partial \psi_i}{\partial x}\dfrac{d}{d\mathbf{q}}\left(\dfrac{\partial x}{\partial \eta}\right) - \dfrac{\partial \psi_i}{\partial y}\dfrac{d}{d\mathbf{q}}\left(\dfrac{\partial x}{\partial \eta}\right)
\end{array}
\right\}
$$

$$
\left\{
\begin{array}{c}
\dfrac{d}{d\mathbf{q}}\left(\dfrac{\partial \phi_i}{\partial x}\right) \\[2mm]
\dfrac{d}{d\mathbf{q}}\left(\dfrac{\partial \phi_i}{\partial y}\right)
\end{array}
\right\}
=
\begin{bmatrix}
\dfrac{\partial x}{\partial \xi} & \dfrac{\partial y}{\partial \xi} \\[2mm]
\dfrac{\partial x}{\partial \eta} & \dfrac{\partial y}{\partial \eta}
\end{bmatrix}^{-1}
\left\{
\begin{array}{c}
-\dfrac{\partial \phi_i}{\partial x}\dfrac{d}{d\mathbf{q}}\left(\dfrac{\partial x}{\partial \xi}\right) - \dfrac{\partial \phi_i}{\partial y}\dfrac{d}{d\mathbf{q}}\left(\dfrac{\partial y}{\partial \xi}\right) \\[2mm]
-\dfrac{\partial \phi_i}{\partial x}\dfrac{d}{d\mathbf{q}}\left(\dfrac{\partial x}{\partial \eta}\right) - \dfrac{\partial \phi_i}{\partial y}\dfrac{d}{d\mathbf{q}}\left(\dfrac{\partial x}{\partial \eta}\right)
\end{array}
\right\}
\tag{17}
$$

$$
\left\{
\begin{array}{c}
\dfrac{d}{d\mathbf{q}}\left(\dfrac{\partial^2 \phi_i}{\partial x^2}\right) \\[2mm]
\dfrac{d}{d\mathbf{q}}\left(\dfrac{\partial^2 \phi_i}{\partial y^2}\right) \\[2mm]
\dfrac{d}{d\mathbf{q}}\left(\dfrac{\partial^2 \phi_i}{\partial x \partial y}\right)
\end{array}
\right\}
=
\begin{bmatrix}
\left(\dfrac{\partial x}{\partial \xi}\right)^2 & \left(\dfrac{\partial y}{\partial \xi}\right)^2 & 2\dfrac{\partial x}{\partial \xi}\dfrac{\partial y}{\partial \xi} \\[3mm]
\left(\dfrac{\partial x}{\partial \eta}\right)^2 & \left(\dfrac{\partial y}{\partial \eta}\right)^2 & 2\dfrac{\partial x}{\partial \eta}\dfrac{\partial y}{\partial \eta} \\[3mm]
\dfrac{\partial x}{\partial \xi}\dfrac{\partial y}{\partial \eta} & \dfrac{\partial x}{\partial \xi}\dfrac{\partial y}{\partial \eta} & \dfrac{\partial x}{\partial \xi}\dfrac{\partial y}{\partial \eta} + \dfrac{\partial x}{\partial \eta}\dfrac{\partial y}{\partial \xi}
\end{bmatrix}^{-1}
\left\{
\begin{array}{c}
b_1 \\ b_2 \\ b_3
\end{array}
\right\}
$$

where b_1, b_2 and b_3 are written as follows.

$$
b_1 = -2\frac{\partial^2 \phi_i}{\partial x^2}\frac{\partial x}{\partial \xi}\frac{d}{d\mathbf{q}}\left(\frac{\partial x}{\partial \xi}\right) - 2\frac{\partial^2 \phi_i}{\partial y^2}\frac{\partial y}{\partial \xi}\frac{d}{d\mathbf{q}}\left(\frac{\partial y}{\partial \xi}\right) - 2\frac{\partial^2 \phi_i}{\partial x \partial y}\left[\frac{d}{d\mathbf{q}}\left(\frac{\partial x}{\partial \xi}\right)\frac{\partial y}{\partial \xi} + \frac{\partial x}{\partial \xi}\frac{d}{d\mathbf{q}}\left(\frac{\partial y}{\partial \xi}\right)\right]
$$

$$
- \frac{d}{d\mathbf{q}}\left(\frac{\partial \phi_i}{\partial x}\right)\frac{\partial^2 x}{\partial \xi^2} - \frac{\partial \phi_i}{\partial x}\frac{d}{d\mathbf{q}}\left(\frac{\partial^2 x}{\partial \xi^2}\right) - \frac{d}{d\mathbf{q}}\left(\frac{\partial \phi_i}{\partial y}\right)\frac{\partial^2 y}{\partial \xi^2} - \frac{\partial \phi_i}{\partial y}\frac{d}{d\mathbf{q}}\left(\frac{\partial^2 y}{\partial \xi^2}\right)
$$

$$
b_2 = -2\frac{\partial^2 \phi_i}{\partial x^2}\frac{\partial x}{\partial \eta}\frac{d}{d\mathbf{q}}\left(\frac{\partial x}{\partial \eta}\right) - 2\frac{\partial^2 \phi_i}{\partial y^2}\frac{\partial y}{\partial \eta}\frac{d}{d\mathbf{q}}\left(\frac{\partial y}{\partial \eta}\right) - 2\frac{\partial^2 \phi_i}{\partial x \partial y}\left[\frac{d}{d\mathbf{q}}\left(\frac{\partial x}{\partial \eta}\right)\frac{\partial y}{\partial \eta} + \frac{\partial x}{\partial \eta}\frac{d}{d\mathbf{q}}\left(\frac{\partial y}{\partial \eta}\right)\right]
$$

$$
- \frac{d}{d\mathbf{q}}\left(\frac{\partial \phi_i}{\partial x}\right)\frac{\partial^2 x}{\partial \eta^2} - \frac{\partial \phi_i}{\partial x}\frac{d}{d\mathbf{q}}\left(\frac{\partial^2 x}{\partial \eta^2}\right) - \frac{d}{d\mathbf{q}}\left(\frac{\partial \phi_i}{\partial y}\right)\frac{\partial^2 y}{\partial \eta^2} - \frac{\partial \phi_i}{\partial y}\frac{d}{d\mathbf{q}}\left(\frac{\partial^2 y}{\partial \eta^2}\right)
\tag{18}
$$

$$
b_3 = \frac{\partial^2 \phi_i}{\partial x^2}\left[\frac{d}{d\mathbf{q}}\left(\frac{\partial x}{\partial \xi}\right)\frac{\partial x}{\partial \eta} + \frac{\partial x}{\partial \xi}\frac{d}{d\mathbf{q}}\left(\frac{\partial x}{\partial \eta}\right)\right] - \frac{\partial^2 \phi_i}{\partial y^2}\left[\frac{d}{d\mathbf{q}}\left(\frac{\partial y}{\partial \xi}\right)\frac{\partial y}{\partial \eta} + \frac{\partial y}{\partial \xi}\frac{d}{d\mathbf{q}}\left(\frac{\partial y}{\partial \eta}\right)\right]
$$

$$
- \frac{\partial^2 \phi_i}{\partial x \partial y}\left[\frac{d}{d\mathbf{q}}\left(\frac{\partial x}{\partial \xi}\right)\frac{\partial y}{\partial \eta} + \frac{\partial x}{\partial \xi}\frac{d}{d\mathbf{q}}\left(\frac{\partial y}{\partial \eta}\right)\right] + \frac{d}{d\mathbf{q}}\left(\frac{\partial x}{\partial \eta}\right)\frac{\partial y}{\partial \xi} + \frac{\partial x}{\partial \eta}\frac{d}{d\mathbf{q}}\left(\frac{\partial y}{\partial \xi}\right)]
$$

$$
- \frac{d}{d\mathbf{q}}\left(\frac{\partial \phi_i}{\partial x}\right)\frac{\partial^2 x}{\partial \xi \partial \eta} - \frac{\partial \phi_i}{\partial x}\frac{d}{d\mathbf{q}}\left(\frac{\partial^2 x}{\partial \xi \partial \eta}\right) - \frac{d}{d\mathbf{q}}\left(\frac{\partial \phi_i}{\partial y}\right)\frac{\partial^2 y}{\partial \xi \partial \eta} - \frac{\partial \phi_i}{\partial y}\frac{d}{d\mathbf{q}}\left(\frac{\partial^2 y}{\partial \xi \partial \eta}\right)
$$